

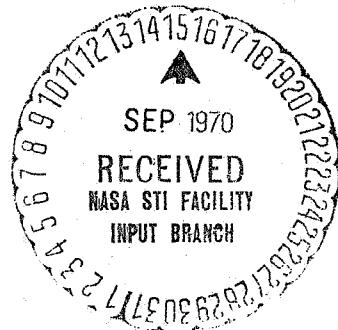
**NASA TECHNICAL  
MEMORANDUM**

Report No. 53924

**DETERMINING THE ORIENTATION OF THE PEGASUS SATELLITES**

By Robert L. Holland, Fred A. Rodrigue and Matthew B. Barkley, Jr.  
Space Sciences Laboratory

September 16, 1969



**NASA**

*George C. Marshall Space Flight Center  
Marshall Space Flight Center, Alabama*

MSFC - Form 3190 (September 1968)

FACILITY FORM 602

<b>N70-75929</b>	(THRU)
(ACCESSION NUMBER)	<i>None</i>
<b>29</b>	(CODE)
(PAGES)	
<i>TMX 53924</i>	(CATEGORY)
(NASA CR OR TMX OR AD NUMBER)	

R-RP-INP-67-2

*msl*

February 28, 1967

This Internal Note was changed to TM X-53924 on September 16, 1969

DETERMINING THE ORIENTATION OF  
THE PEGASUS SATELLITES

by

Robert L. Holland, Fred A. Rodrigue,  
and Matthew B. Barkley, Jr.

PHYSICS AND ASTROPHYSICS BRANCH  
RESEARCH PROJECTS LABORATORY

## ABSTRACT

The collection of data and their analytical reduction required to orient the Pegasus satellites are described. Since earth-fixed axes are accurately related in space and time to the sun and other celestial bodies, Pegasus body-fixed axes are space-fixed by orienting them with the space-fixed earth axes.

Earth and sun vectors are established in Pegasus-fixed and earth-fixed coordinates as the basis for the analysis. Earth-fixed values are determined from ephemerides, and Pegasus-fixed values are determined from data telemetered from the solar aspect and infrared sensors on the satellites.

An understanding of the design, orientation, and application of Pegasus sensors is essential for the correct use of the sensor data. Corrected interpretation of Gray-coded sun-sensor calibration is explained. The analytic means are described for reducing probable error, which is a result mainly of the large angle subtended by the earth disk, in the earth vector.

Relationships of Pegasus body axes and of earth-fixed axes to an intermediate coordinate system are formulated as two matrices. The product of one matrix with the transpose of the second is a matrix suitable for transforming any vector in Pegasus body-fixed coordinates to earth-fixed coordinates. In addition, a method is described for calculating the satellites' weighted average angular momentum vector.

## TABLE OF CONTENTS

Section	Page
I. INTRODUCTION	1
II. CALCULATION OF SPACE-FIXED VECTORS	1
III. CALCULATION OF BODY-FIXED VECTORS	4
A. Calculation of the Sun Vector	6
B. Calculation of the Earth Vector	14
IV. CALCULATION OF THE SATELLITE ORIENTATION	19
V. AVERAGE OF THE SPIN-AXIS VECTORS	20
REFERENCES	24

## LIST OF ILLUSTRATIONS

Figure		Page
1	Space-Fixed and Orbit-Plane Coordinate Systems	2
2	Pegasus Body-Fixed Coordinate System	5
3	Solar Aspect Sensor	7
4	Coordinate Systems for Calculating Sensor-Fixed Sun Vector	9
5	Arrangement of Solar Aspect Sensors	12
6	Simplified View of Infrared Sensor Head	15
7	Coordinate System Used to Improve Satellite-Earth Vector $\hat{R}'$	18

## I. INTRODUCTION

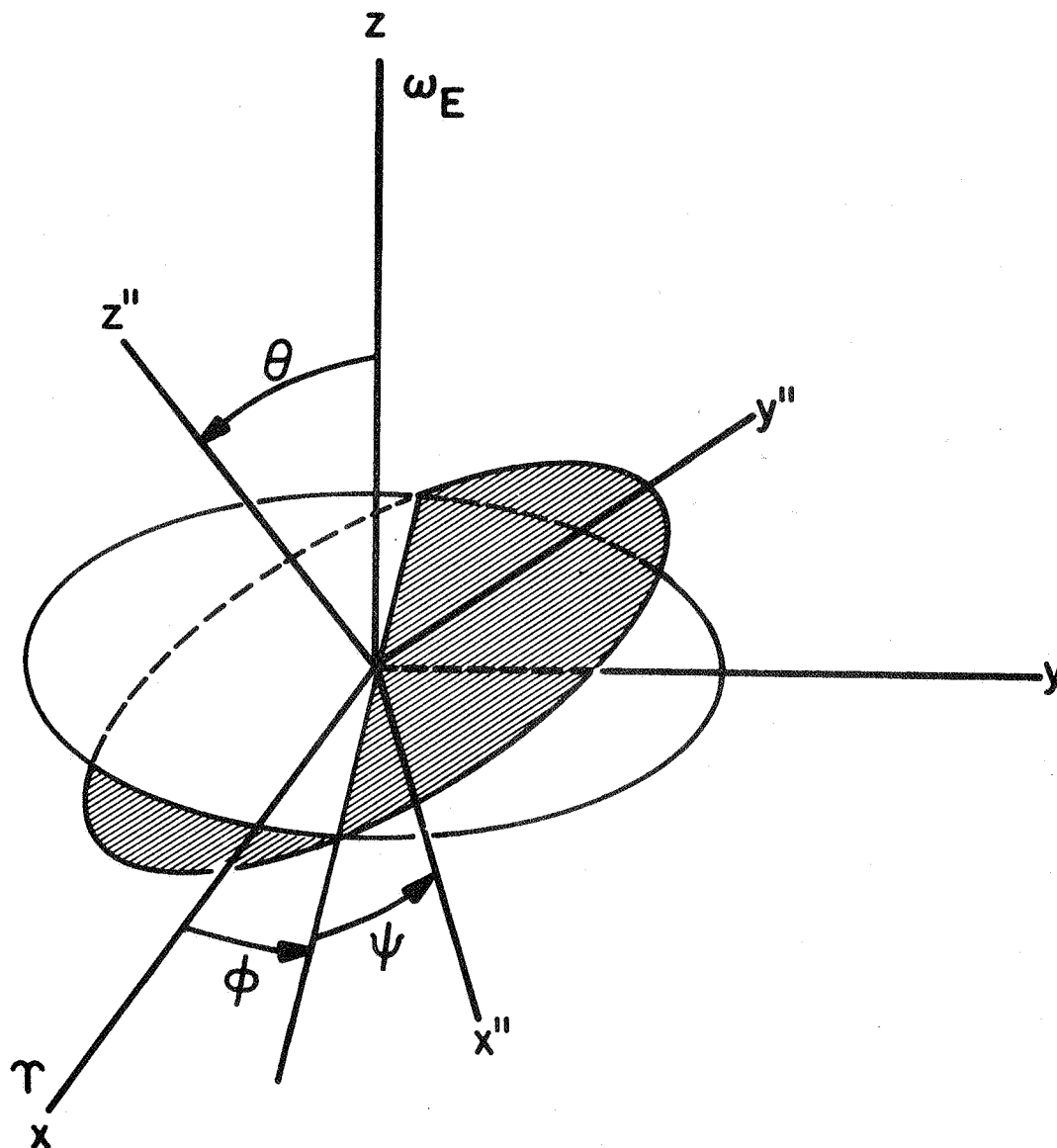
When a directional analysis of Pegasus meteoroid data was planned, installation of an attitude sensing system on the Pegasus satellite, for determining satellite orientation, became imperative. The reduced probabilities of meteoroid impact due to earth shielding can be estimated by knowing only the satellite's position in orbit. But the analysis is much more meaningful if one also knows the direction a detection panel is facing when a hit occurs. In addition, analysis of data from radiation sensors on board the satellite can be refined if sensor orientation is known.

The motion of the satellite was itself a significant problem. At the time of launch, little theoretical work had been done on the rotational motion of rigid bodies in orbit having differing moments of inertia about each of the three principal axes; for example, almost all researchers had assumed two of the moments of inertia to be equal. The Pegasus satellites afforded an opportunity to formulate and check a theory of this particular kind of rotational motion.

This paper deals with only one aspect of the investigation, the reduction of Pegasus data to meaningful numbers. The method of calculating the instantaneous orientation, and a way of finding values of the average angular momentum vector are described. Both types of data are being compiled into ephemerides which will be published.

## II. CALCULATION OF THE SPACE-FIXED VECTORS

This section outlines the calculation of the space-fixed earth and sun vectors. Space-fixed as commonly used means that vectors are located in a geocentric equatorial coordinate system. The direction of the vernal equinox is the reference direction, and the earth's equatorial plane is the reference plane (Fig. 1). Since only the directions of the



$x, y, z$  are space-fixed coordinates.  
 $x'', y'', z''$  are orbit-plane coordinates.  
 $\tau$  is the vernal equinox at some date.  
 $x$ - $y$  is the earth equatorial plane.  
 $\theta, \phi, \psi$  are conventional Euler angles.  
 $\omega_E$  is the earth's spin vector.

FIGURE 1. SPACE-FIXED AND ORBIT-PLANE COORDINATE SYSTEMS

vectors are important here, all vectors are normalized to unit length. As a reminder to the reader, each unit vector is identified by a cap (^).

The vector  $\hat{S}$  pointing from the earth to the sun can be found in any relevant solar ephemeris. This is considered the same as the vector pointing from the satellite to the sun, since the 0.003-degree parallax between them is negligible.

The space-fixed unit earth vector  $\hat{R}$ , which points from earth center to satellite center, is calculated from satellite tracking data using equations developed with the following orbital elements:

$T_0$  = epoch time (time to which all position measurements are referred)

$\Omega_0$  = right ascension of ascending node at  $T_0$

$\dot{\Omega}$  = rate of change of  $\Omega$  (regression of nodes)

$i$  = inclination of the orbit plane to the earth equatorial plane (very nearly constant)

$\omega_0$  = argument of perigee at  $T_0$

$\dot{\omega}$  = rate of change of  $\omega$  (advance of perigee)

$M_0$  = mean anomaly at  $T_0$

$N_0$  = mean motion (angular orbital speed) at  $T_0$

$\dot{N}$  = rate of change of mean motion

$e$  = eccentricity

To obtain the space-fixed earth vector  $\hat{R}$ , an earth vector  $\hat{R}''$  is first calculated in a coordinate system having the perigee direction of the satellite orbit as the reference direction and the orbit plane as its reference plane (see Fig. 1). Quantities in this system are denoted by double-primed letters. Then  $\hat{R}$  is obtained by transforming  $\hat{R}''$  into space-fixed coordinates.

The mean anomaly  $M$  is the angle which is the product of mean angular velocity of the satellite and the elapsed time after some specified epoch time  $T_0$ .

$$M = M_0 + N_0 (t - T_0) + \frac{1}{2} \dot{N} (t - T_0)^2 \quad 0 \leq M < 2\pi$$

The eccentric anomaly  $E$  can be derived by successive approximations, using the calculated value of  $M$ , the ephemeris value of  $e$ , and Kepler's equation (relating the mean and eccentric anomalies):

$$E = M + e \sin E$$

The true anomaly, angle  $V$ , locating the satellite at time  $t$ , is derived from the geometry of the elliptic orbit as:

$$V = 2 \tan^{-1} \left[ \left( \frac{1+e}{1-e} \right)^{\frac{1}{2}} \tan \frac{E}{2} \right]$$

Then, in the orbit plane,

$$\hat{R}'' = \begin{bmatrix} \cos V \\ \sin V \\ 0 \end{bmatrix}$$

The Euler angle matrix  $[A^{-1}]$  given in Goldstein [1] may be used to transform the orbit-plane coordinates of the satellite-earth unit vector to space-fixed coordinates after the following identifications are made:

$$\begin{aligned} \phi &= \Omega_0 + \dot{\Omega} (t - T_0) & 0 \leq \phi < 2\pi \\ \theta &= i & 0 \leq \theta \leq \pi \\ \psi &= \omega_0 + \dot{\omega} (t - T_0) & 0 \leq \psi < 2\pi \end{aligned}$$

$$\text{Then } \hat{R} = [A^{-1}] \hat{R}''$$

Computation of the space-fixed vectors  $\hat{S}$  and  $\hat{R}$  requires no observations from the satellite itself; thus, they can never give the satellite's orientation. Their accuracy, however, is much greater than the vectors obtained from satellite sensor data. This fact will be applied later as a means of improving on the raw data obtained from the satellite sensors.

### III. CALCULATION OF THE BODY-FIXED VECTORS

Two independent vectors have been established based upon observations from the earth. To determine satellite orientation, measurements for calculating these vectors must be made from the satellite. The coordinate system used is shown in Figure 2. The chosen axes correspond



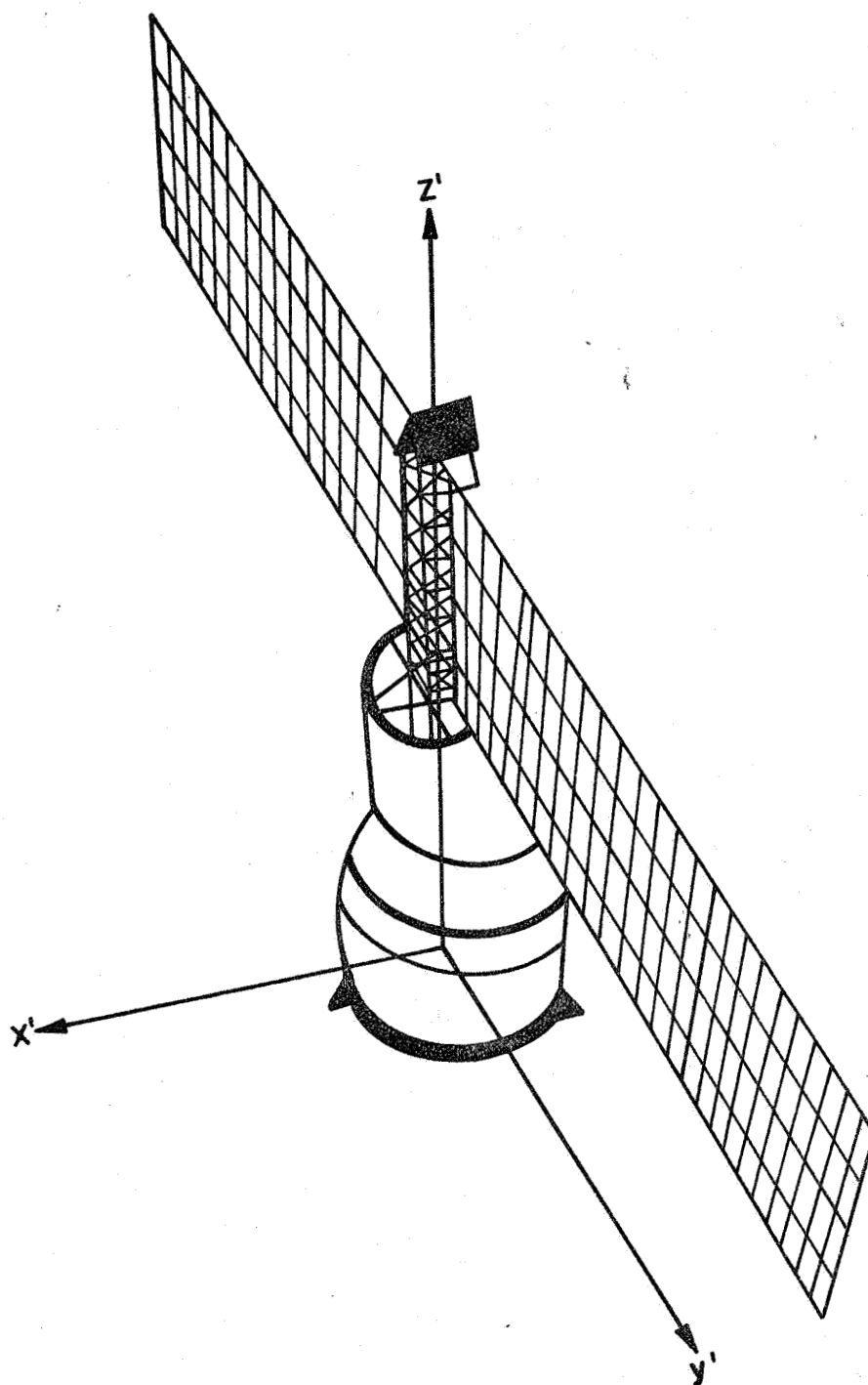


FIGURE 2. PEGASUS BODY-FIXED COORDINATE SYSTEMS

to the principal axes of the body:  $x'$  is the axis of the maximum moment of inertia,  $z'$  is the axis of the minimum moment of inertia, and  $y'$  is the axis of the intermediate moment of inertia. (All body-fixed quantities are denoted by primed letters.) Knowledge of the sun and earth vectors in the body-fixed system and in the space-fixed system will enable a determination of the relationship of the body-fixed coordinate system to the space-fixed coordinate system. Application of this relationship to the body-fixed coordinates gives the desired space orientation of the body.

#### A. Calculation of the Sun Vector

Data for the calculation of the body-fixed sun vector  $\hat{S}'$  are telemetered from Pegasus as the output of any of five sun sensors. The sun vector is found first in sensor coordinates  $x^*$ ,  $y^*$ ,  $z^*$  for an individual sensor and then transformed into body-fixed coordinates. Since the design of the sensors determines how the sensor-fixed sun vector is calculated, a brief description of the device is given.

##### 1. General Description of the Sun Sensor

Each sun sensor is a small aluminum block (5.7 cm by 5.7 cm by 1 cm) containing two aspect sensors at right angles to each other [2]. The aspect sensor (Fig. 3) is an oblong block of fused quartz having a slit centered along its top surface, and a Gray-coded reticle and seven photosensitive strips on its bottom surface.

The reticle consists of an opaque surface with rectangular clear areas patterned to transmit sunlight selectively to the photocells beneath. Light passes through the slit, casting a narrow band of illumination across the seven rows of clear areas. Thus seven bits of information reading respectively "yes" or "no" are given as sunlight either passes through a reticular aperture and energizes a photocell, or is blocked by an opaque area. The illustration shows a typical sun ray entering an aspect sensor and being refracted at the surface of the quartz block. The "sheet" of

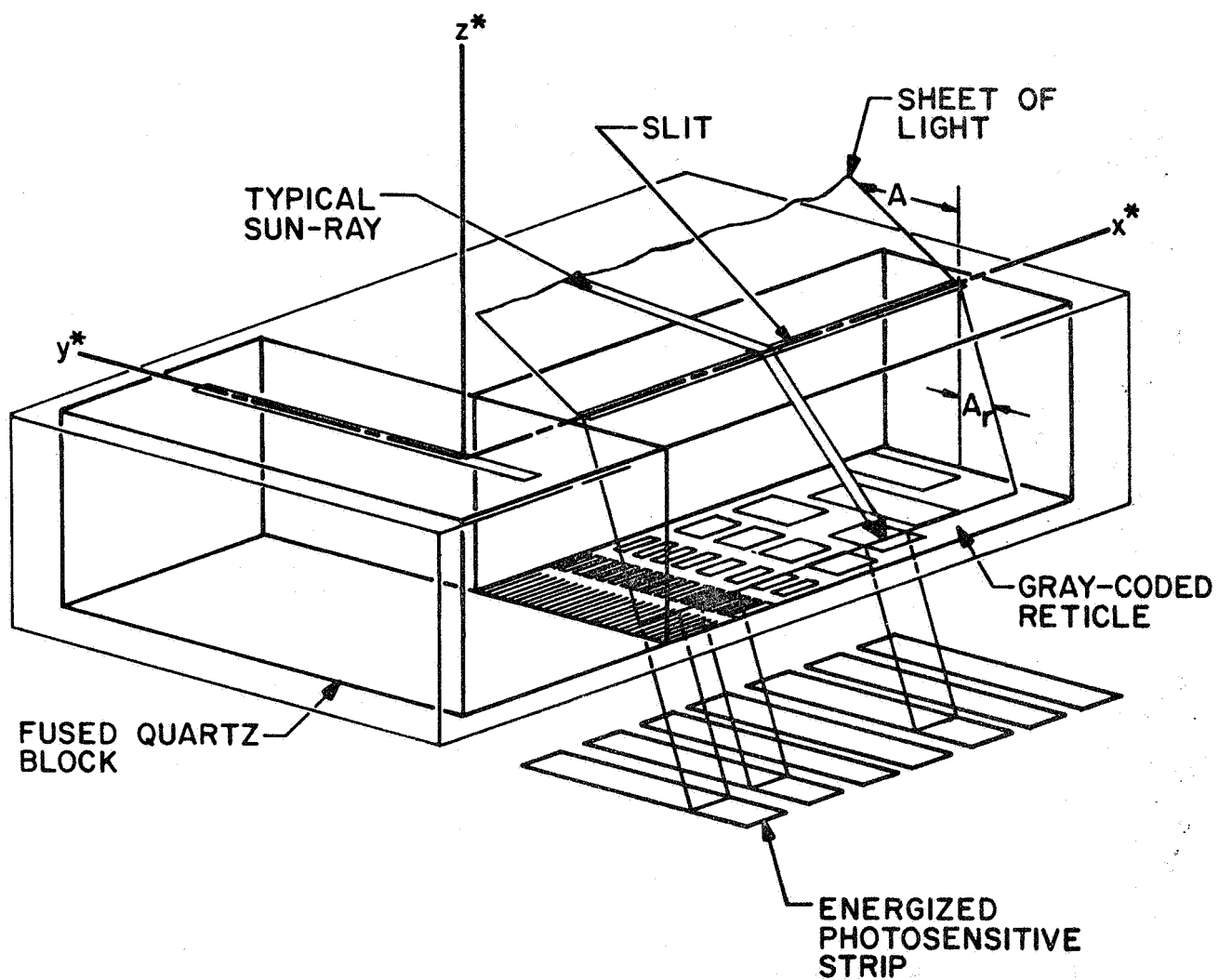


FIGURE 3. SOLAR ASPECT SENSOR

sunlight above the block is composed of the rays "selected" by the slit from the total incident beam of light and transmitted after refraction into the quartz. The slit is sufficiently long that the sets of openings at the ends of the reticle are never in shadow while the sun sensor is operating within the design field of view.

The Gray-code output signals of a sensor can be converted to binary and thence to decimal numbers of degrees. Sensor output signal is a function of angle  $A_r$  in Figure 3. The calibration process used rays incident normal to the slit, having a range of  $+63.5^\circ$  to  $-63.5^\circ$  in increments of  $1^\circ$  for angle  $A$ , for values of  $A$  related to  $A_r$  by Snell's Law:

$$\sin A = \eta \sin A_r \quad (\text{true only for rays normal to slit})$$

where  $\eta$  is the refractive index of quartz. The calibration process represents an error in analytic approach to sensor application. The error is explained and compensated for in the analytic methods for general data reduction developed in the following subdivisions of this section. The Gray-coded pattern is used because it permits a movement of the area of illumination to cause a change in light transmission through only one aperture at a time. Thus, only one bit can change at a time. The use of a pattern reading directly in binary, however, would usually require more than one-bit change for a one-degree change in angle. Any imperfections in the pattern would result in nonsynchronous bit changes, and could cause catastrophic errors in angle determinations.

## 2. Derivation of Basic Sun Sensor Relations

The sensor-fixed sun vector  $S^*$  (Fig. 4) is located when its angle of incidence  $i_s$  and the angle  $\theta_s$  are determined. (The angle  $\theta_s$  is the angle in the  $x^*-y^*$  plane which the "vertical" plane containing the incident and refracted rays makes with the  $x^*$  axis.)

The quantities  $i_s$  and  $\theta_s$  can be derived from the angles  $A_r$  and  $B_r$  (Figs. 3 and 4). Angles  $A_r$  and  $B_r$  are the orthogonal projections in the quartz sensor block of the angle of refraction  $r_s$  of the refracted sun vector  $S_r^*$ .

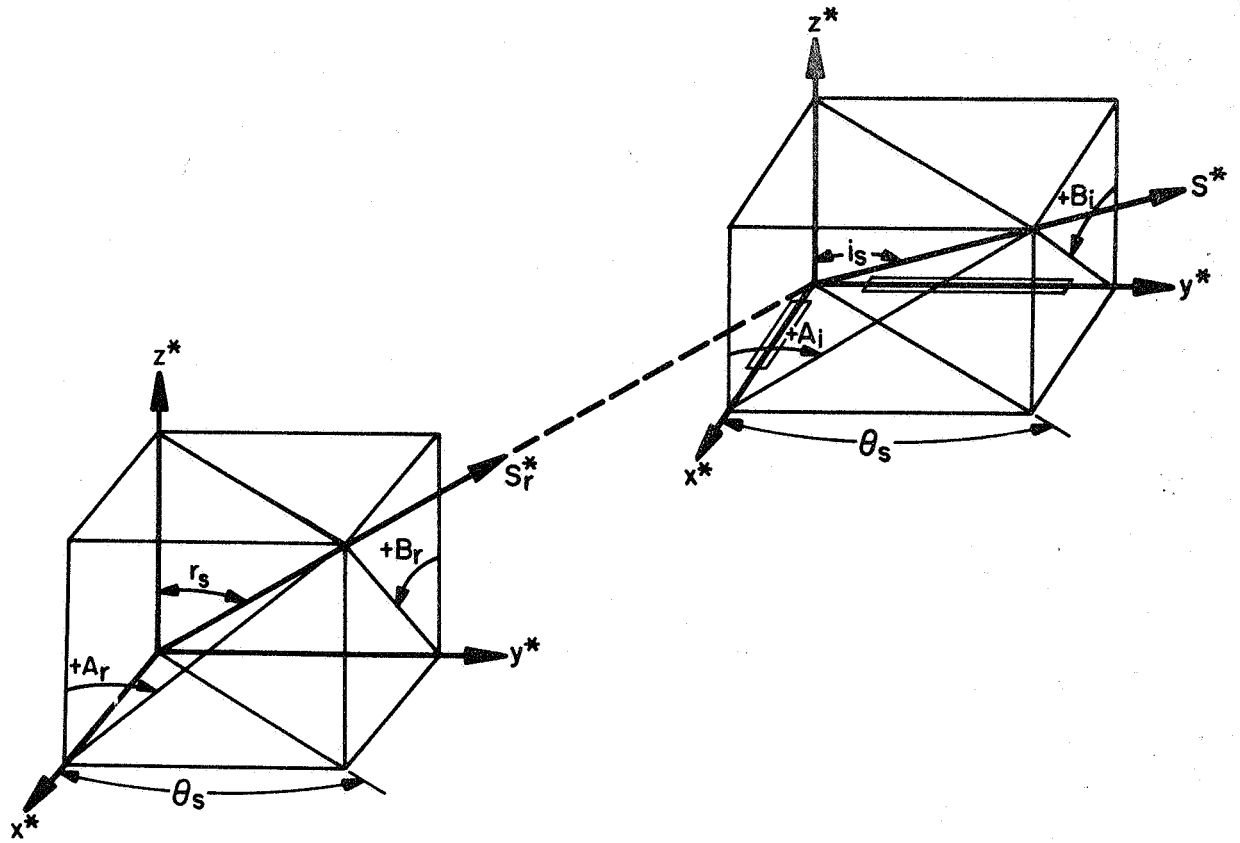


FIGURE 4. COORDINATE SYSTEMS FOR CALCULATING  
SENSOR-FIXED SUN VECTOR

(Note that for convenience in Figure 4 the incident sun vector  $S^*$  and its refracted portion  $S_r^*$  are located by two displaced but mutually parallel and equivalent sets of  $x^*$ ,  $y^*$ , and  $z^*$  coordinates.)

In Figure 4,  $S_{r_z}^* \tan B_r$  and  $S_{r_z}^* \tan A_r$  are the projections of  $S_{r_z}^* \tan r_s$  in the  $z^* - y^*$  and  $z^* - x^*$  planes, respectively. According to the Pythagorean Theorem:

$$(S_{r_z}^*)^2 \tan^2 r_s = (S_{r_z}^*)^2 \tan^2 B_r + (S_{r_z}^*)^2 \tan^2 A_r \quad (1)$$

$$\text{hence } r_s = \arctan(\tan^2 A_r + \tan^2 B_r)^{\frac{1}{2}} \quad (2)$$

According to Snell's Law,  $\sin i_s = \eta \sin r_s$ , where  $\eta$  is the refractive index of the quartz sensor block;

$$\text{therefore, } i_s = \arcsin(\eta \sin r_s) \quad (3)$$

and  $\tan \theta_s = S_{r_z}^* \tan A_r / S_{r_z}^* \tan B_r$  (Fig. 4), hence

$$\theta_s = \arctan(\tan A_r / \tan B_r) \quad (4)$$

The rectangular components of  $S^*$  are:

$$S_x^* = \sin i_s \cos \theta_s$$

$$S_y^* = \sin i_s \sin \theta_s$$

$$S_z^* = \cos i_s$$

Thus equations (2), (3), and (4) are sufficient to locate the sun vector  $S^*$  if  $A_r$ ,  $B_r$ , and  $\eta$  are known.

Angles  $A_r$  and  $B_r$  are obtained from the telemetered data points  $A_a$  and  $B_a$  derived from the relations

$$A_r = \arcsin(\sin A_a / \eta) \quad (5)$$

$$B_r = \arcsin(\sin B_a / \eta) \quad (6)$$

(Angles  $A_a$  and  $B_a$  in equations (5) and (6) have no physical significance but are used to correct for the error introduced by the sensor design and calibration as explained in subdivision A4, Explanation and Correct Application of Sun Sensor Calibration.)

### 3. Transformation of Sun Vector to Pegasus Body Coordinates

As shown in Figure 5, the sun sensors are arranged on the satellite with their surfaces parallel to the faces of an imaginary square pyramid whose center is at the satellite's center of mass. From pre-launch measurements the exact orientation of each sensor relative to the satellite is known. The orientation of the  $k$ th sensor is expressed as a matrix  $\begin{bmatrix} W_k \end{bmatrix}$  which transforms any vector in the  $x^*$ ,  $y^*$ , and  $z^*$  coordinates for sensor  $k$  to Pegasus body coordinates  $x'$ ,  $y'$ , and  $z'$ :

$$S' \equiv \begin{bmatrix} S'_x \\ S'_y \\ S'_z \end{bmatrix} = \begin{bmatrix} W_k \end{bmatrix} \begin{bmatrix} S^*_x \\ S^*_y \\ S^*_z \end{bmatrix} \quad (7)$$

Thus the sun vector in body coordinates  $S'$  is obtained.

### 4. Explanation and Correct Application of Sun Sensor Calibration

It is apparent that the use of Snell's Law in equations (5) and (6) nullifies the prior application of this law during calibration of the sun sensors, as previously explained in Section III A. Equations (5) and (6) are needed because of an error in design and calibration of the sensor Gray-code strips. The design was based upon the mistaken premise that the projections of the incident angle  $i_s$  in the  $x^*-z^*$  and  $y^*-z^*$  planes (angles  $A_i$  and  $B_i$ ) are related to  $A_r$  and  $B_r$  by Snell's Law. However it will be shown that this premise is not true, that is,

$$\sin A_i \neq \eta \sin A_r = \sin A_a \quad (8)$$

$$\sin B_i \neq \eta \sin A_r = \sin B_a \quad (9)$$

This non-equality is apparent from geometric considerations, and may be demonstrated as follows. The equality in equation (8) is squared:

$$\sin^2 A_r = \sin^2 A_a / \eta^2 \quad (10)$$

According to a basic trigonometric relation:

$$\cos A_r = (1 - \sin^2 A_r)^{\frac{1}{2}} \quad (11)$$

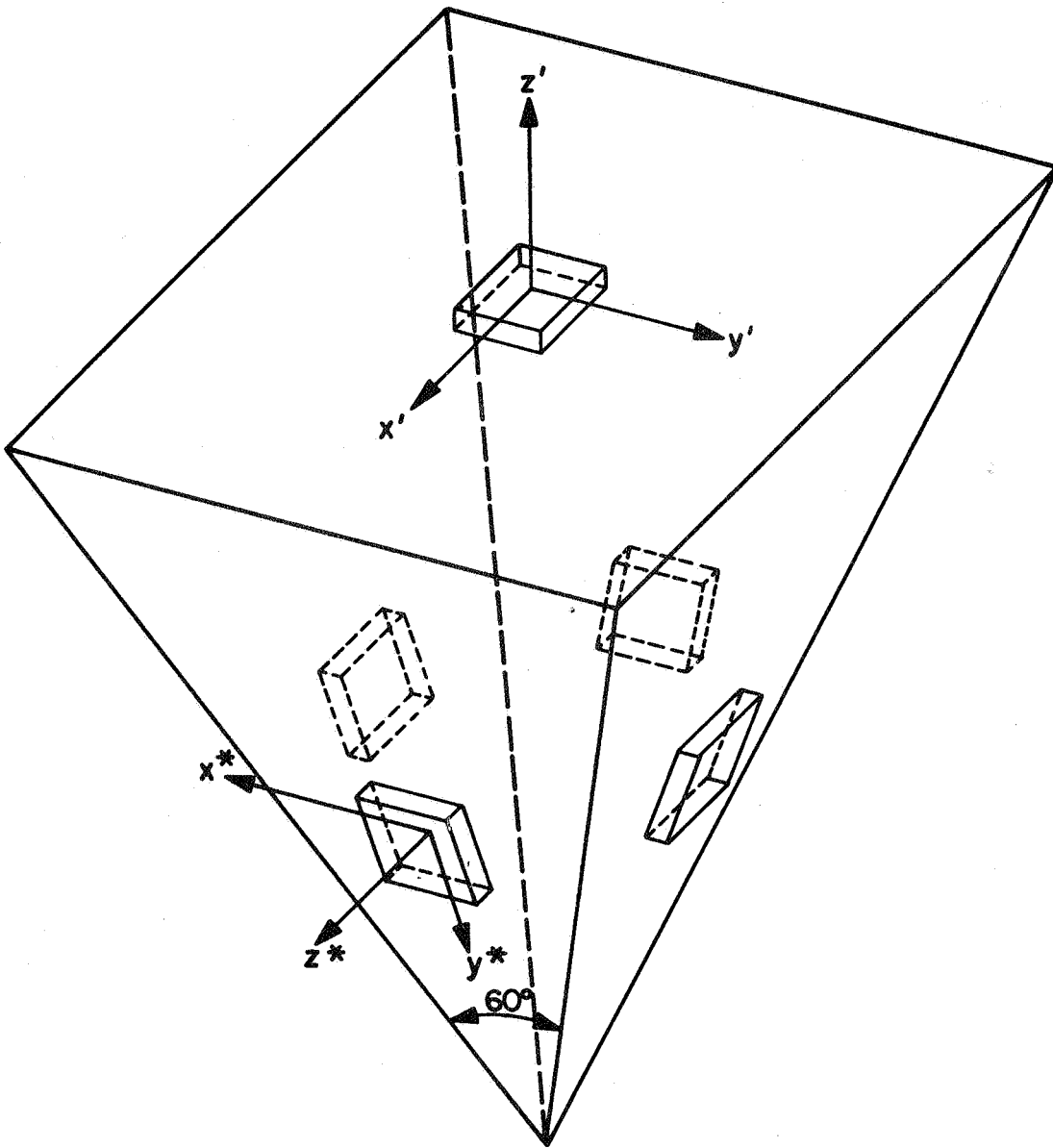


FIGURE 5. ARRANGEMENT OF SOLAR ASPECT SENSORS



Equation (10) is substituted in equation (11):

$$\cos A_r = \left(1 - \frac{\sin^2 A_a}{\eta^2}\right) = \frac{(\eta^2 - \sin^2 A_a)^{\frac{1}{2}}}{\eta} \quad (12)$$

Similarly,

$$\cos B_r = \frac{(\eta^2 - \sin^2 B_a)^{\frac{1}{2}}}{\eta} \quad (13)$$

$$\text{and } \tan \alpha = \frac{\sin \alpha}{\cos \alpha} = \frac{\sin \alpha}{(\eta^2 - \sin^2 \alpha)^{\frac{1}{2}}} \quad (14)$$

where  $\alpha = A_a$ , or  $B_a$ , or  $A_r$ , or  $B_r$ .

In reference to Figure 4, if  $A_a = A_i$ , and  $B_a = B_i$ , then

$$\tan \theta_s = \frac{S_{rz}^* \tan A_r}{S_{rz}^* \tan B_r} = \frac{S_{rz}^* \tan A_a}{S_{rz}^* \tan B_a} \quad (15)$$

$$\text{or } \frac{\tan A_r}{\tan B_r} = \frac{\tan A_a}{\tan B_a} \quad (16)$$

Values of equations (12), (13), and (14) are substituted in equation (16):

$$\begin{aligned} \frac{\frac{\sin A_a}{(\eta^2 - \sin^2 A_a)^{\frac{1}{2}}/\eta}}{\frac{\sin B_a}{(\eta^2 - \sin^2 B_a)^{\frac{1}{2}}/\eta}} &= \frac{\frac{\sin A_a}{(1 - \sin^2 A_a)^{\frac{1}{2}}}}{\frac{\sin B_a}{(1 - \sin^2 B_a)^{\frac{1}{2}}}} \quad (17) \end{aligned}$$

With the equation further simplified the non-equality is apparent (since  $\eta_{\text{quartz}} = 1.5$ ):

$$\frac{\eta^2 - \sin^2 A_a}{\eta^2 - \sin^2 B_a} \neq \frac{1 - \sin^2 A_a}{1 - \sin^2 B_a} \quad (18)$$

and hence  $A_a \neq A_i$ , and  $B_a \neq B_i$ ; therefore equation (16) is false.

Initial reduction of Pegasus sun sensor telemetry data was erroneous because the original calibration and the instructions for data reduction were based upon the incorrect application of Snell's Law indicated above. The error appeared as sine wave components in data-point plots, which indicated satellite nutation. However, analysis showed no valid

reason for such motion. When data points were corrected through the use of equations (5) and (6) to obtain  $A_r$  and  $B_r$ , thence  $\theta_s$  and  $r_s$ , and through use of Snell's Law to obtain  $i_s$  from  $r_s$ , the major irregularities were removed. Plots of the revised data points were smoothest for  $\eta = 1.455$ ; therefore, this value of  $\eta$  has been used.

The authors are grateful to Dr. Leland Cunningham, Astronomy Department, University of California, for interpreting the source of error.

This subdivision has presented a description of the sun sensor system and has shown how it is used to find the sun vector in body coordinates. The next subsection deals with the body-fixed earth vector,  $\hat{R}'$ , the last consideration necessary before the satellite orientation can be found.

#### B. Calculation of the Earth Vector

This subsection describes the earth sensor system, how the earth vector is calculated, and how its accuracy is improved.

The earth vector  $\hat{R}'$  in body coordinates points from the satellite's center to the earth's center. The earth is located from Pegasus by means of six infrared sensor tubes (Fig. 6). The sensor output signals are recorded and subsequently telemetered (on demand) to earth where the data are used to calculate the satellite body-fixed unit vector  $\hat{R}'$ . Each tube points normal to opposite faces of an imaginary regular dodecahedron centered in the satellite. Radiation may enter through the germanium lens at either end of the sensor tube. When the temperature difference across the thermopile exceeds the predicted differential between earth and space (212°K), the "hot" end of the tube is considered to be "on." The earth's disk subtends an angle of about 127° at apogee and about 134° at perigee; thus, at any one time, three to six sensors will "see" the earth.

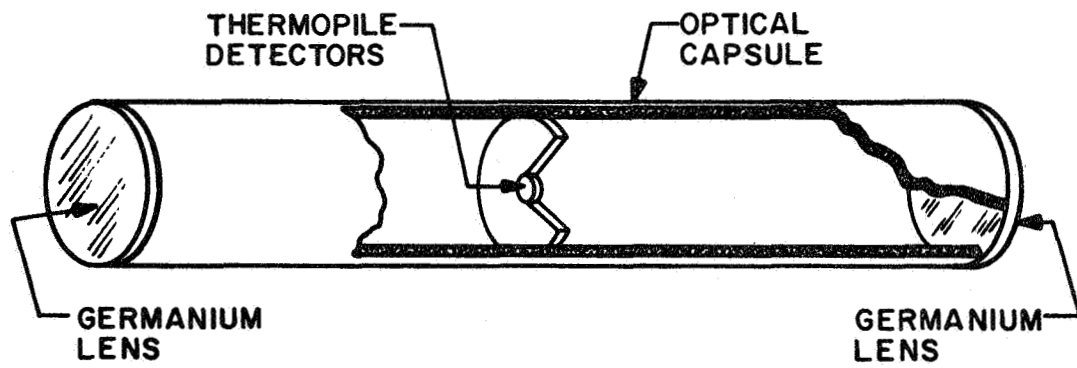


FIGURE 6. SIMPLIFIED VIEW OF INFRARED SENSOR HEAD

Each "on" sensor defines a vector  $\hat{H}_k'$  directed along its sensor-tube axis. As noted above, the tubes radiate with uniform angular distribution around a satellite center. Hence the three to six sensors which are "on" at any instant will tend to have vectors  $\hat{H}_k'$  more or less uniformly distributed within the cone subtending the earth disk. Therefore a best value of earth vector  $\hat{R}'$  is obtained by adding and normalizing the vectors for the three to six "on" sensors:

$$\hat{R}' = \frac{\sum \hat{H}_k'}{|\sum \hat{H}_k'|} \quad (19)$$

Because only six sensor tubes are used,  $\hat{R}'$  has a 50 percent chance of pointing  $20^\circ$  or more away from the earth's center. The 3.5-degree field of view of each sensor further limits the accuracy of  $\hat{R}'$ . However, there is a method of improving the accuracy of vector  $\hat{R}'$ , and it is explained as follows.

The sun vectors alone cannot give the complete orientation of Pegasus, because they can supply only two of the three Euler angles needed. However, the earth vector measurements also supply two angles, providing one more than is necessary. Thus, the system is over-determined, and this allows an extra restriction on  $\hat{R}'$ ; that is, the accuracy of vectors  $\hat{S}$ ,  $\hat{R}$ , and  $\hat{S}'$  is much better than that of  $\hat{R}'$ , and the following relationship should be true:

$$-\hat{R} \cdot \hat{S} = \hat{R}' \cdot \hat{S}' \quad (20)$$

(Because of the way the earth vectors are defined,  $\hat{R}'$  should equal  $-\hat{R}$  in the same coordinate system.) If equation (20) is not true, one may assume that the fault lies almost entirely with  $\hat{R}'$ . Then  $\hat{R}'$  may be corrected to comply with the restriction that equation (20) imposes.

This may be done by rotating  $\hat{R}'$  in the plane formed by  $\hat{R}'$  and  $\hat{S}'$  until equation (20) holds, that is, until the angle between  $\hat{R}'$  and  $\hat{S}'$  is the same as the angle  $\alpha_s$  between  $-\hat{R}$  and  $\hat{S}$ :

$$\alpha_s = \arccos(-\hat{R} \cdot \hat{S}) \quad (21)$$

The rotation takes place in a new coordinate system  $C_1, C_2, C_3$ , defined by  $\hat{R}'_C$  and  $\hat{S}'$  (Fig. 7):

$$C_1 = \begin{bmatrix} m_{11} \\ m_{21} \\ m_{31} \end{bmatrix} = \hat{S}' \quad (22)$$

$$C_2 = \begin{bmatrix} m_{12} \\ m_{22} \\ m_{32} \end{bmatrix} = \frac{(\hat{S}' \times \hat{R}'_C) \times \hat{S}'}{|(\hat{S}' \times \hat{R}'_C) \times \hat{S}'|} \quad (23)$$

$$C_3 = \begin{bmatrix} m_{13} \\ m_{23} \\ m_{33} \end{bmatrix} = \frac{\hat{S}' \times \hat{R}'_C}{|\hat{S}' \times \hat{R}'_C|} \quad (24)$$

where  $m_{ij}$  is the  $i$ th direction cosine of the  $C_j$  axis. Since the angle between  $\hat{R}'$  and  $\hat{S}'$  should be  $\alpha_s$ , the corrected components of  $\hat{R}'$  in this system should be:

$$\begin{bmatrix} \cos \alpha_s \\ \sin \alpha_s \\ 0 \end{bmatrix} \quad (25)$$

The  $C_3$  component is zero because the  $C_3$  axis is normal to the plane of  $\hat{R}'$  and  $\hat{S}'$ . Now the three sets of  $m_{ij}$  may be used to form a matrix which will transform the new vector back to body coordinates:

$$\hat{R}'_C = \begin{bmatrix} m_{11} & m_{12} & m_{13} \\ m_{21} & m_{22} & m_{23} \\ m_{31} & m_{32} & m_{33} \end{bmatrix} \begin{bmatrix} \cos \alpha_s \\ \sin \alpha_s \\ 0 \end{bmatrix} \quad (26)$$

Vector  $\hat{R}'$  points somewhere in a region containing the actual direction from satellite to earth center. The refined vector  $\hat{R}'_C$  points somewhere along an arc in that region; this arc also contains the actual satellite-earth direction.

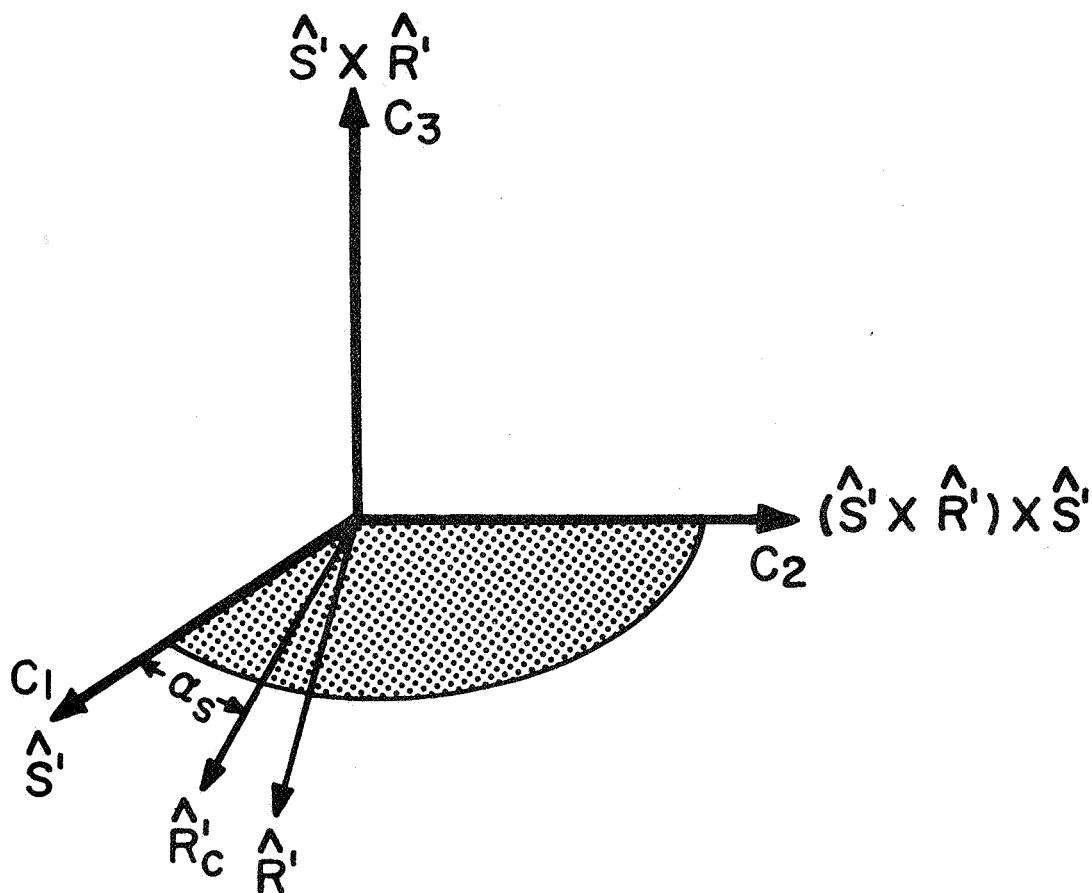


FIGURE 7. COORDINATE SYSTEM USED TO IMPROVE SATELLITE-EARTH VECTOR  $\hat{R}'$

#### IV. CALCULATION OF THE SATELLITE ORIENTATION

As stated earlier, finding the orientation of a body means finding the direction, in a space-fixed system, of each body axis. The relationship between body-fixed and space-fixed axes may be expressed as a transformation matrix  $[T]$  which transforms any vector  $\hat{G}'$  in body coordinates to an equivalent vector  $\hat{G}$  in space coordinates:

$$\hat{G} = [T] \hat{G}' \quad (27)$$

The desired matrix is found by constructing a set of intermediate coordinates  $X_I$ ,  $Y_I$ , and  $Z_I$ . These are used to calculate transformation matrices  $[B]$ , which transforms a vector from body to intermediate coordinates, and  $[A]$ , which transforms a vector from space to intermediate coordinates. The desired transformation matrix is:

$$[T] = [A] [B^t] \quad (28)$$

The detailed calculation is as follows. An intermediate coordinate system based on  $\hat{S}$  and  $\hat{R}$  is constructed:

$$X_I = \begin{bmatrix} a_{11} \\ a_{21} \\ a_{31} \end{bmatrix} = \hat{S} \quad (29)$$

$$Y_I = \begin{bmatrix} a_{12} \\ a_{22} \\ a_{32} \end{bmatrix} = \frac{(\hat{S} \times \hat{R}) \times \hat{S}}{|(\hat{S} \times \hat{R}) \times \hat{S}|} \quad (30)$$

$$Z_I = \begin{bmatrix} a_{13} \\ a_{23} \\ a_{33} \end{bmatrix} = \frac{\hat{S} \times \hat{R}}{|\hat{S} \times \hat{R}|} \quad (31)$$

The same is done for  $\hat{S}'$  and  $\hat{R}'$ :

$$X'_I = \begin{bmatrix} b_{11} \\ b_{21} \\ b_{31} \end{bmatrix} = \hat{S}' \quad (32)$$

$$Y_I' = \begin{bmatrix} b_{12} \\ b_{22} \\ b_{32} \end{bmatrix} = \frac{(\hat{S}' \times \hat{R}_C' \times \hat{S}')}{|(\hat{S}' \times \hat{R}_C') \times \hat{S}'|} \quad (33)$$

$$Z_I' = \begin{bmatrix} b_{13} \\ b_{23} \\ b_{33} \end{bmatrix} = \frac{\hat{S}' \times \hat{R}_C'}{|\hat{S}' \times \hat{R}_C'|} \quad (34)$$

Although only one intermediate system was mentioned previously, two have been constructed. The x-z planes of these two intermediate coordinate systems can be assumed to be parallel within good limits of accuracy. The x-y planes, however, are parallel within the poor limits of accuracy attributable to the unimproved earth-sensor vector of equation (19). To use the information gathered so far, we must assume that the coordinate systems are identical.

Any vector in the intermediate system is represented by  $\hat{G}_I$ , thus:

$$\hat{G} = [A] \hat{G}_I \quad (35)$$

$$\text{and } \hat{G}' = [B] \hat{G}_I$$

$$\text{therefore } [B^t] \hat{G}' = \hat{G}_I \quad (36)$$

since  $[B]$  is an orthogonal matrix.

Equation (36) is substituted in equation (35):

$$\hat{G} = [A] [B^t] \hat{G}' \quad (37)$$

Thus the transformation matrix expressed in equation (28) has been derived:

$$[T] = [A] [B^t] \quad (38)$$

## V. AVERAGING OF AXIS VECTORS

The theoretical methods which treat the motion of Pegasus [3] predict the direction of the angular momentum vector (that is, the spin axis). An ephemeris of the spin vector calculated from observations was necessary to verify the theoretical methods, but the unweighted average of observations



failed to give a reasonably smooth ephemeris plot. Therefore, data-point observations of spin-axis direction were statistically smoothed to obtain an ephemeris of the angular momentum vector. At the time of this writing Pegasus A is spinning about the x body axis, while Pegasus B and Pegasus C are spinning about the z body axis.

Theory predicts for the angular momentum vector a regular path in so-called orbit-plane coordinates, a system having the direction of ascending node as its reference direction and the orbit plane as its reference plane. For this reason, the spin-axis vector is transformed from space-fixed to orbit-plane coordinates for smoothing, and then transformed back to space-fixed coordinates for ephemeris insertion.

The transformation to orbit-plane coordinates is done, as in Section II, by means of a Euler angle matrix. The current value of the ascending node is  $\phi$ :

$$\phi = \Omega = \Omega_0 + \dot{\Omega} (t-t_0) \quad 0 \leq \phi < 2\pi$$

The constant value of the inclination is  $\theta$ :

$$\theta = i \quad 0 \leq \theta \leq \pi$$

And the argument of perigee is ignored, so that

$$\psi = 0$$

The transformation matrix [P] is used for transforming from space to orbit-plane axes and is defined as follows:

$$[P] = \begin{bmatrix} \cos \Omega & \cos i \sin \Omega & \sin i \sin \Omega \\ -\sin \Omega & \cos i \cos \Omega & \sin i \cos \Omega \\ 0 & -\sin i & \cos i \end{bmatrix} \quad (39)$$

Each of the Pegasus body-fixed axes can be considered as a space-fixed vector. For example,

$$\hat{Z}_b = [T] \hat{Z}' \quad (40a)$$

where  $\hat{Z}_b$  is the space-fixed vector pointing in the direction of the Z body axis, and  $\hat{Z}' = (0, 0, 1)$  is the body-fixed version of the same vector. With similar definitions,

$$\hat{X}_b = [T] \hat{X}' \quad (40b)$$

All quantities in the orbit-plane system are double-primed:

$$\hat{Z}_b'' = (P) \hat{Z}_b \quad \text{or} \quad \hat{X}_b'' = (P) \hat{X}_b \quad (41)$$

The process for smoothing spin-axis data in order to develop a Pegasus angular-momentum ephemeris is considered next. Spin axis  $\hat{Z}_b''$  for Pegasus B and Pegasus C is used in the development which follows. (Spin axis  $\hat{X}_b''$  may of course be substituted for specific application to Pegasus A.)

Data telemetered from Pegasus is used for calculating the successive orbital point values of spin-axis attitude  $\hat{Z}_b''$ . Transmissions occur at two different rates:

- 1) at 5-minute intervals (normal mode)
- 2) at  $2\frac{1}{2}$ -second intervals (rapid attitude mode)

Point values of  $\hat{Z}_b''$  may be expressed as follows:

$$\begin{aligned} \hat{Z}_{b \text{ normal}}'' &= \hat{Z}_{bn}'' \\ \hat{Z}_{b \text{ rapid}}'' &= \hat{Z}_{br}'' \end{aligned}$$

For each full minute of rapid attitude mode (or fraction of a minute at the beginning and end), an unweighted average of  $\hat{Z}_{br}''$  values is calculated:

$$\bar{Z}_{br}'' = \frac{\sum \hat{Z}_{br}''}{|\sum \hat{Z}_{br}''|} \quad (42)$$

The  $\bar{Z}_{br}''$  averages from rapid attitude and  $\hat{Z}_{bn}''$  vectors from normal mode are accumulated for a 6-hour interval, then averaged together:

$$\bar{Z}_b'' = \frac{\sum \bar{Z}_{br}'' + \hat{Z}_{bn}''}{|\sum (\bar{Z}_{br}'' + \hat{Z}_{bn}'')|} \quad (43)$$

About fifty vectors go into this average; thus, statistical smoothing methods are applicable. Equation (43) is used as an initial average to find the angle  $\beta_k$  between the average  $\bar{Z}_b''$  and the individual vectors:

$$\beta_k = \arccos (\hat{Z}_b'' \cdot \hat{Z}_{bk}'') \quad (44)$$

where  $\hat{Z}_{bk}''$  represents either a value of  $\hat{Z}_{br}''$  from equation (42) or a value of  $\hat{Z}_{bn}''$ , and  $k$  goes from 1 to about 50. The actual angular-momentum vector should move regularly and not too quickly (neglecting any sudden perturbations). The angle  $\beta_k$  may be assumed to have a random (that is, Gaussian) distribution around the average  $\beta_k$ . The average  $\beta_k$  represents the vertex half-angle of the cone that the spin vector makes as it precesses around the angular-momentum vector. The average is calculated:

$$\bar{\beta} = \frac{\sum \beta_k}{N} \quad N = \text{maximum value of } k$$

and the root mean square deviation:

$$\sigma = \left( \frac{\sum (\beta_k - \bar{\beta})^2}{N} \right)^{\frac{1}{2}}$$

Smoothing is now applied. If  $\beta_k > 2\sigma$  for any  $k$ , a new average is calculated as in equation (43), omitting vectors for which  $\beta_k$  is too large. Then a new set of  $\beta_k$ , a new average, and a new  $\sigma$  are calculated and the test is repeated. This is continued until no more vectors can be eliminated. The final average is the desired answer, and all that remains is to transform it back to space:

$$\hat{Z}_b = [P^t] \hat{Z}_b'', \text{ where } [P^t] \text{ is the transposed matrix of } [P].$$

## REFERENCES

1. Goldstein, H., Classical Mechanics. Addison-Wesley Publ. Co., Inc., 1950; pp. 107-109.
2. Anon., Adcole Digital Solar Aspect Systems. Adcole Corp.
3. Holland, R.L., A First Order Theory and Applications for the Rotational Motion of a Triaxial Rigid Body Orbiting an Oblate Primary. A Thesis, University of Alabama, 1967.

## DISTRIBUTION

### R-RP

E. Stuhlinger  
G. Heller  
J. Downey  
J. Dozier  
R. Shelton  
G. Arnett  
H. Atkins  
T. Bannister  
M. Barkley (15)  
T. Calvert  
S. Clifton  
D. Cochran  
J. Cortez  
B. Duncan  
P. Espy  
B. Ferguson  
S. Fields  
J. Fountain  
W. Fountain  
J. Harrison  
R. Hembree  
R. Holland (15)  
B. Jones  
R. Lal  
R. Linton  
R. Merrill

J. Michlovic  
E. Miller  
D. Mitchell  
W. Moore  
R. Naumann  
W. Neely  
J. Reynolds  
C. Schafer  
W. Snoddy  
C. Swanson  
P. Tashbar  
J. Watkins  
H. Weathers  
D. Wilkes  
H. Williams  
J. Williams  
F. Wills  
E. Wright  
J. Zwiener  
Reserve (5)

### R-AERO-FT

R. Benson  
E. Fleischman  
P. Rebels

### R-COMP-RRF

F. Rodrigue

### MS-IP